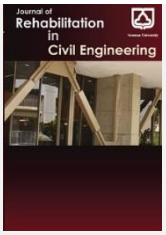

Journal of Rehabilitation in Civil Engineering

Journal homepage: https://civiljournal.semnan.ac.ir/

Assessment of the Magnetic Field Influence on the Mechanical, Durability and Microstructural Properties of Concrete Containing Silica Fume

Fakhri Javahershenas [1]; Malek Mohammad Ranjbar [2,*]; Morteza Sohrabi Gilani [3]; Mohammad Hajforoush [4]

1. Ph.D. Student, Department of Civil Engineering, University of Guilan, Rasht, Iran
2. Professor, Department of Civil Engineering, University of Guilan, Rasht, Iran
3. Ph.D., Department of Civil Engineering, University of Guilan, Rasht, Iran
4. Postdoctoral, Department of Civil Engineering, University of Guilan, Rasht, Iran

* Corresponding author: ranjbar@guilan.ac.ir

ARTICLE INFO

Article history:
Received: 03 May 2025
Revised: 03 June 2025
Accepted: 16 June 2025

Keywords:
Magnetic field;
Concrete;
Silica fume;
Durability;
SEM.

ABSTRACT

The present experimental research aims to evaluate the effect of applying directly magnetic flux densities of 0.5, 0.8 and 1 Tesla (T) to fresh concrete specimens containing 5 and 10% silica fume (SF). Regarding this, compressive and flexural strengths tests were used to assess the mechanical properties of the concrete. Furthermore, durability, of concrete specimens exposed to magnetic fileds (MFs) was investigated using the electrical resistance and chloride ion penetration tests. In order to analyze the microstructure of concrete, scanning electron microscopy (SEM) images were taken from concrete specimens subjected to MFs. Finally, a method has been introduced to determine the flexural strength of concrete under the influence of MF, relying on its cylinder compressive strength. According to this study observations, optimal results were achieved through MF of 1 T and 10% SF replacement. Hence, applying MF of 1 T to concrete specimens incorporating 10% SF enhanced their compressive, flexural and electrical strengths by 24, 15 and 18%, respectively. Following this, depth of chloride ions penetration was decreased by 15%. The SEM analysis revealed that the microstructure of concrete exposed to MF becomes denser and less porous, supporting the mechanical and durability findings.

E-ISSN: 2345-4423

How to cite this article:
Javahershenas, F., Ranjbar, M. M., Sohrabi Gilani, M. and Hajforoush, M. (2026). Assessment of the Magnetic Field Influence on the Mechanical, Durability and Microstructural Properties of Concrete Containing Silica Fume. Journal of Rehabilitation in Civil Engineering, (),

1. Introduction

In recent decades, a significant number of researches have been performed on the mechanical properties and durability of cementations composites incorporating pozzolanic materials like silica fume (SF), but not many on their conductivity property. According to the literature, the inclusion of SF as a partial replacement of binder in concrete improves its mechanical and durability properties [1,2]. The SF particles are very small and have a high percentage of SiO2 content, which act with calcium hydroxide (Ca(OH)2) and form finally calcium silicate hydrates (C-S-H) gel in cementations composites manufacturing [3–5]. Therefore, the utilization of SF in concrete can strongly enhance its durability especially in aggressive environments since the capillary porosity and permeability of concrete decreased by adding SF to it [6,7]. Following this, Celik et al. [8] probed the effect of using various percentages of SF on the mechanical performance of concrete. They reported that adding 5% SF to concrete can increase compressive, splitting tensile and flexural strengths of concrete by 11, 8 and 6%, respectively. Garg et al. [9] examined the effect of using SF in concrete on its mechanical strength and electrochemical corrosion probability. The results indicated that the adding 12% SF to concrete specimens increased their compressive strength by about 18%, and decreased the corrosion probability of concrete by 32%. Ahmad et al. [10] surveyed the coefficients of chloride ion diffusion in concrete containing 5% SF. They concluded that the presence of SF in concrete improved its water penetration and coefficients of chloride diffusion up to 58 and 86 %, respectively. Additionally, the use of waste materials in cementations composites can reduce the carbon footprint and CO2 emissions in concrete industry [11,12]. Recently, a few studies have been conducted in order to increase the mechanical properties of cementitious composites by profiting from magnetism phenomenon. Besides, there are not enough researches on durability of concrete exposed to magnetic fields (MFs). As per previous studies, the effect of MF on concrete specimens can be considered as two aspects. Applying of MF to mixing water of concrete strongly improved the mechanical properties and workability of different kinds of concrete [13,14]. As known, water polar molecules have opposite ends carrying opposite charges [15]. Following this, the MF can readily influence the physical properties of water such as viscosity, temperature, electric conductivity, pH, solubility, specific weight, surface tension and permeability pressure [15–18]. Regarding this, Hamed et.al [16] evaluated the effect of using magnetized water on mechanical properties of geopolymer concrete containing SF. Their results showed that using magnetized water in preparing the alkaline activator of geopolymer concrete increased its compressive and flexural strengths by about 64 and 41%, respectively. Gholhaki et al. [19] evaluated the influence of magnetized water on the properties of self-compacting concrete containing different pozzolans. They found that magnetized water enhanced compressive strength of concrete up to 18%. Furthermore, Su et al. [20,21] reported that the MF treated water can reduce the cement consumption in concrete up to 5%, and improve the microstructure of concrete by forming more C-S-H gel in the cement hydration process.

According to various recent researches, the application of MF to fresh cementitious composites increased mainly their mechanical properties [22,23,32–39,24–31]. Soto-Bernal et al. [22] revealed that compressive strength of cement paste subjected to the MF increased by 13%. In addition, Abavisani et al. [23] showed that the applying MF of 0.5 Tesla (T) to concrete with steel chips increased its mechanical strength by about 17%. Also, tensile strength of cement mortar containing steel fibers exposed to MF was surveyed by Ferrandez et al. [24]. They demonstrated that MF can increase its strength up to 10%. Abavisani et al. [27] showed that the applying MF to concrete beams enhanced their load-bearing capacity by 7%. Furthermore, the study performed by Rezaifar et al. [26] clarified that compression behavior of reinforced concrete columns exposed to MF was improved by about 11%. Safari tarbozagh et al. [30] indicated the effect of MF on mechanical strength of concrete specimens with carbon nanotubes. The results showed that the applying 0.5 T MF to concrete with 0.04% carbon nanotubes can enhance its compressive strength by 11%. Hajforoush et al. [31] assessed the effect of applying MF to concrete with

steel fibers. Their results showed that the applying MF to concrete enhanced its mechanical strength by about 18%. Hajforoush et al.[32,33] in another studies reported that the microstructure of concrete exposed to MF became less porous and denser. Javahershenas et al. [34] evaluated the effect of MF exposure time on the performance of concrete containing steel fibers. They concluded that the applying MF for 2 minutes to the concrete enhanced its compressive and flexural strengths by about 20 and 27%, respectively. Recently, researchers evaluated the effect of different MF intensities on engineering properties of concrete. Concerning this, Amini et al. [37] probed the compressive strength of concrete specimens incorporating silica sand and SF compositions exposed to MF of 0.5 and 1 T. The results showed that an increase in MF intensity has a notable effect on compressive strength of concrete specimens. Following this, the applying MF of 1 T to concrete specimens containing 10% silica sand and SF caused an increase about 8.5% in their compressive strength, compared to the same specimens with MF of 0.5 T. Rezaifar et al. [38] conducted the same experimental study on concrete specimens incorporating nano silica and steel fibers exposed to MF. Regarding this, applying MF of 0.5 and 1 T to concrete specimens with 1% steel fibers and 10% nano silica can increase their compressive strength up to 26 and 43%, respectively. Ahmad and Manar [39] investigated the effect of applying different MF intensities on compressive strength of concrete specimens. They evaluated compressive and tensile strengths of concrete specimens subjected to MFs (25, 50, 100, 200, 400 and 500 mT). The results clarified that the optimum MF intensity was 400 mT, increasing in mechanical strength of concrete by about 29%.

Exposing ready-mixed concrete to a magnetic field (MF) affects its hardened performance in aggressive environments. Since there are not enough and efficient studies on the durability characteristics of concrete subjected to MFs, this study focused on their mechanical, durability and microstructural properties of concrete containing silica fume (SF) as a partial binder replacement. The study aims to use magnetic fields to enhance the performance of concrete in corrosive environments. Up to the author's knowledge, there are not efficient studies dealing with the influence of applying different MF intensities to fresh concrete specimens incorporated with different percentages of SF on their microstructure and durability properties in aggressive environments. The present study evaluated the durability of concrete subjected to the different MF intensities in a chloride environment for the first time. Most research on the use of MFs in the concrete industry has prioritized studying how cement-based composites behave mechanically when exposed to MFs. This indicates that there is no study on durability of concrete incorporating SF, which was subjected to different MF intensities. Hence, the present study investigates the influence of applying MF of 0.5-1 Tesla (T) directly to fresh concrete specimens with SF (5% and 10% by weight of binder) on their microstructure, mechanical properties and durability particularly. In this paper, durability characteristics of concrete with SF subjected to MF are investigated by using electrical resistance and chloride ion penetration tests in an aggressive environment. In addition, microstructure of concrete specimens incorporating SF exposed to the different MF intensities is assessed by means of scanning electron microscopy (SEM) imaging. Furthermore, compressive and flexural strengths tests are employed to investigate the mechanical performance of concrete specimens at the ages of 7-90 days. Finally, an equation has been offered to assess the flexural strength of concrete subjected to the different MF intensities based on their compressive strengths results. Then, the proposed equation is compared to those recommended by ACI 318-19 [40] for plain concrete. In order to generate MF, a permanent magnetic system was developed to achieve the desired densities (0.5-1 T), consisting of two neodymium magnets compared to two current-carrying coils.

2. Experimental investigation and tests procedure

2.1. Materials

In order to elaborate concrete specimens, Portland cement, SF, fine and coarse aggregates, water and superplasticizer were utilized. Type II Portland cement based on the requirement of ASTM C150 [41] was employed where its properties are given in Table 1. SF was used as a partial replacement of binder in concrete specimens (5% and 10% by weight of binder). It acts as diamagnetic particles, and its properties are presented in Table 1. With respect to ASTM C33 [42], fine aggregate with a particle size range of 0-6 mm and coarse aggregate with a maximum size of 15 mm were utilized. The size distributions of river sand and crushed gravel are depicted in Fig. 1. The main physical properties of river sand and crushed gravel are listed in Table 2. The characteristics of mixing water employed in the experiments was based on ASTM D1129 [43]. In the present study, a carboxylate-based superplasticizer was used, as specified by ASTM C494 [44]. Its specific gravity was measured at 1.11 g/cm³, and its pH level was determined to be 7.

Table 1. Properties of cement and SF.

Physical characteristics	Density (g/cm^3)	Blaine fitness (cm^2/g)	Initial setting time (min)	Final setting time (min)
Cement	3.15	3055	165	255

Chemical composition (% by weight)	SiO_2	Al_2O_3	Fe_2O_3	CaO	MgO	SO_3	K_2O	Na_2O
Cement	22.45	4.85	3.95	64.86	0.8	0.85	0.51	0.25
SF	94.4	0.73	0.21	0.28	0.17	0.45	0.24	0.11

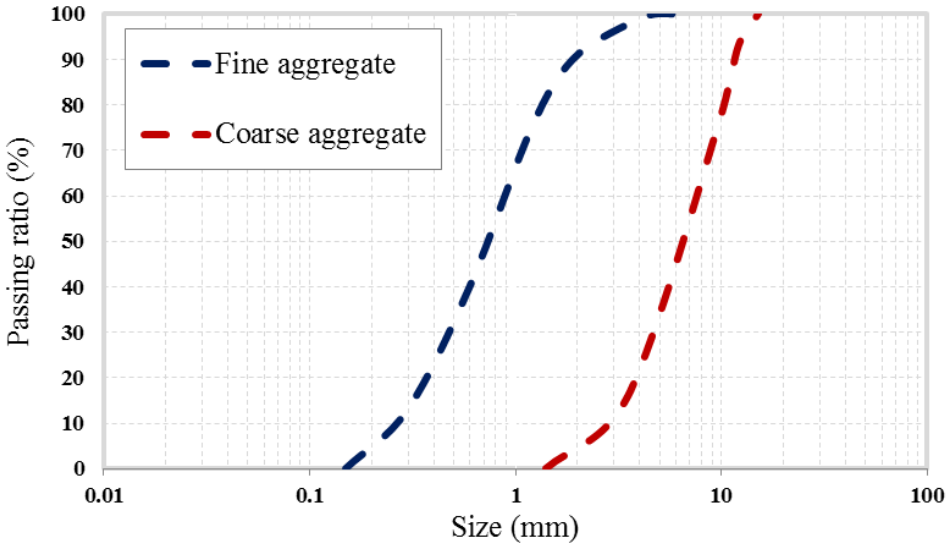

Fig. 1. The size distributions of river sand and crushed gravel.

Table 2. Properties of river sand and crushed gravel [34].

Properties	Fine aggregate	Coarse aggregate
Specific density (g/cm^3)	2.6	2.65
Water content (%)	2.28	1.05
Fitness modulus	2.6	-
Shape	Round	Angular
Surface texture	Smooth	Rough

2.2. Electromagnetic device employed: explanations and calculations

Electric current in a coil generates MF, which is more concentrated in the center of the circular loop [32]. The direction of MF at the center of the circular loop is perpendicular to plane of the loop, as depicted in Fig. 2. The magnitude of MF at the center of a current carrying circular loop of copper wire is determined by Eq. (1) [45]:

$$dB = \frac{\mu I dL \times r}{4\pi R^2} \quad (1)$$

where B is MF in Tesla (T), $\mu = \mu_r \mu_0$ is the magnetic permeability of the material measured in T.m/A, μ_r is the relative permeability, and $\mu_0$is the permeability of free space with the amount of $4\pi \times 10^{-7}$T.m/A. I is current in loop in amperes (A), r is vector between each point along the loop and the field point and R is radius of loop in meters (m). According to the outer product of two vectors dL and r, the Eq. (1) can be written as Eq. (2):

$$dB = \frac{\mu I dL sin\theta}{4\pi R^2} \quad (2)$$

where θ is the angle between electric current and magnetic field which is always equal to 90° for a circular loop. Therefore, the Eq. (2) is modified as Eq. (3) as shown below:

$$B = \frac{\mu I}{4\pi R^2} \oint dL \quad (3)$$

Since electric current rounds just through the circumference of the circular loop with a radius R, Eq. (4) can be written as follows:

$$\oint dL = 2\pi R \quad (4)$$

Finally, MF at the center of a coil of copper wire is calculated by Eq. (5) as shown below:

$$B = \frac{\mu I}{2R} \quad (5)$$

For a circular coil of wire consisting of N turns, the Eq. (5) is changed to Eq. (6) as follows:

$$B = \frac{\mu N I}{2R} \quad (6)$$

In the present study, in order to generate MF of flux densities 0.5 to 1 T and to minimize thermal losses, electromagnetic coils were designed and established in collaboration with neodymium magnets (NdFeB N52), which generate magnetic flux in the same direction. For this purpose, a strong U-shaped iron core and a movable metal plate have been used to adjust the displacement, allowing for a range from 50 to 300 mm to accommodate different samples of various dimensions. The plate can be easily moved by a drive shaft. There are N52 permanent magnets on both sides of the plates, which can generate a magnetic flux of 0.5 T. Furthermore, two bobbins of the coil were manufactured and coated with 600 turns of copper wire with a diameter of 1 mm around the iron core to increase the field intensity in alignment with the MF generated by the magnets. The generated setup is covered with an aluminum sheet. The current utilized to produce the desired MF ranged from 1 to 6 A, generated by a power supply with an electrical potential difference of up to 22 V. The electromagnetic setup used in the present paper is depicted in Fig. 3. To generate a magnetic field with an intensity of 1 T under experimental conditions, a combination of magnets and current-carrying coils was used. Magnetic fields exceeding 1 T have no practical application due to human effects and also findings from conducted studies [22,23,32–39,24–31]. Therefore, in practical applications, the desired field can be generated based on structural requirements and by considering various factors influencing the magnetic field including electric current, magnetic

permeability of the material, and element dimensions. High-intensity MFs may pose risks to users; therefore, in the present study, protective equipment was installed on the device alongside operational guidelines to ensure user safety. Specific measures include implementing an residual-current device to prevent accidental short circuits, coating copper wires with air-dry insulating varnish, and installing an aluminum casing with 1.5 mm thickness to contain magnetic field dispersion beyond the device while concentrating it within the space between the U-shaped plate and permanent magnets. The details of the setup employed in the present study are shown in Fig. 4. A uniform MF can be observed between the opposing poles of two magnets or within a current-carrying coils. This uniform MF arises when two opposite poles are positioned closely together. MFs consistently flow from the North pole to the South pole [45].

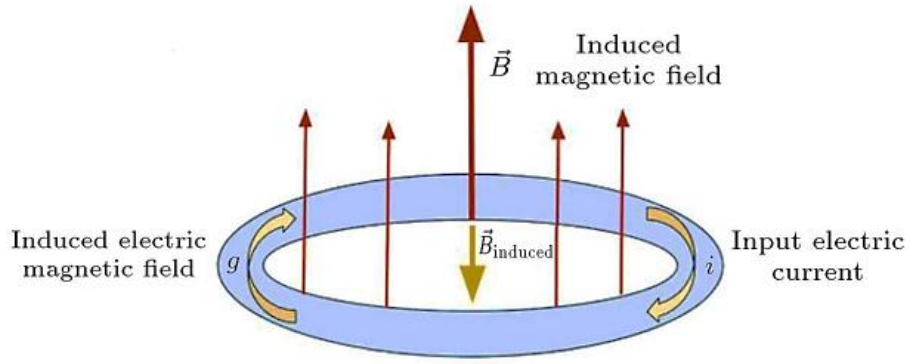

Fig. 2. The pattern of the magnetic flux lines around the current-carrying circular loop [24].

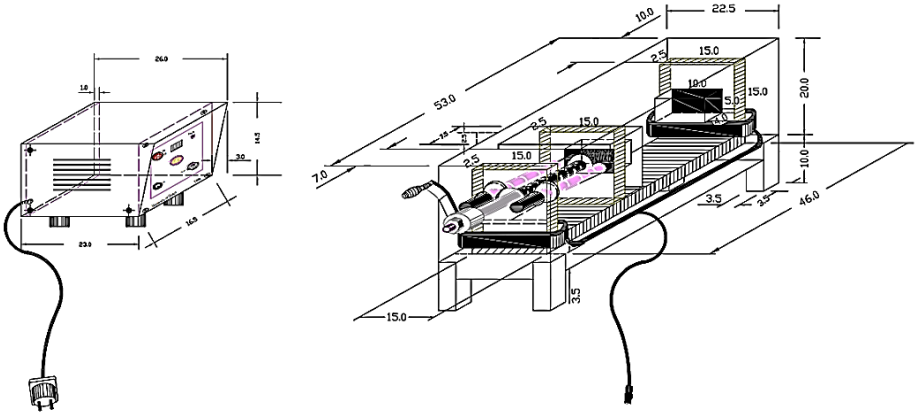

Fig. 3. Electromagnetic device schematic diagram used in the present study.

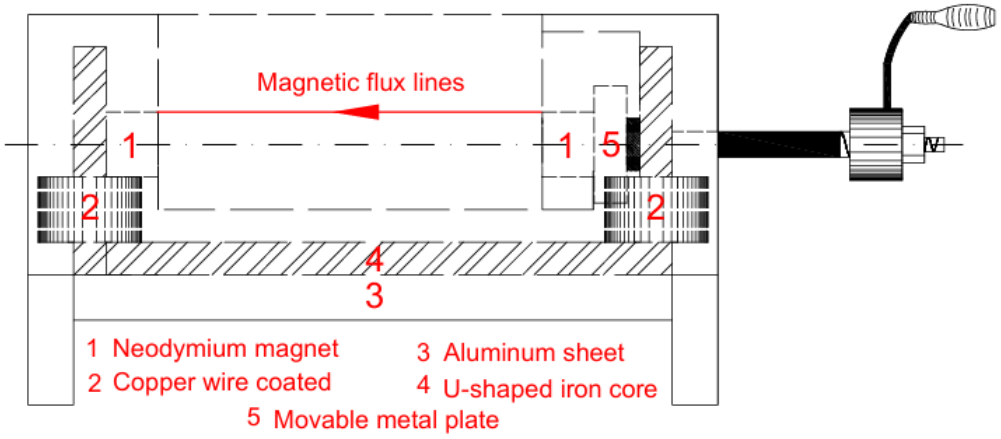

Fig. 4. Detailed setup employed in the present study.

2.3. Experimental procedure

In the present study, to investigate mechanical performance of concrete samples incorporating 0, 5 and 10% SF, as recommended by previous researchers [8,9], compressive and flexural strengths tests were conducted at the ages of 7-90 days. Electrical resistance of concrete, rapid chloride penetrability test (RCPT) and rapid chloride migration test (RCMT) were carried out to assess the durability of concrete specimens. The microstructure of concrete incorporating SF, which were exposed to different MF intensities, was analyzed by means of SEM imaging. Regarding this, compression test was performed on 100 mm cube, while flexural and electrical strengths tests were performed on 70 x 70 x 280 mm prism concrete specimens. In addition, RCPT and RCMT were carried out on 100 x 200 mm cylinder specimens. Following this, concrete specimens containing 0, 5 and 10% SF were classified into four categories: Non-Magnetized concretes without SF (N.Mag), which were not exposed to MF, Magnetized concretes without SF (Mag), which were exposed to MF upon casting fresh concrete specimens into molds for 2 minutes, Non-Magnetized specimens with 5 and 10% SF (N.Mag-SF5or10), which were not exposed to MF and also Magnetized concretes with 5 and 10% SF (Mag-SF5or10), which were exposed to the MF upon casting concrete specimens into molds for 2 minutes. To achieve the objectives of the experimental research, mix proportion of concrete specimens with respect to ASTM C192 [46] is presented in Table 3. The experimental concrete samples were cured in water tanks until the testing days. As shown in Fig. 5, the magnetized concrete specimens were exposed to the MF of 0.5, 0.8 and 1 T for 2 minutes as recommended by previous studies [30–32]. It should be noted that for the present study, preliminary tests were performed to determine the optimal flux densities and exposure time. In the device fabrication process, the specifications of the copper wire were selected such that a 2-minute current flow would not generate heat considerably. Hence, applying the magnetic field to the concrete had no effect on the temperature of the specimens.

Table 3. Mix proportion of concrete specimens.

Water (kg/m^3)	Fine aggregate (kg/m^3)	Coarse aggregate (kg/m^3)	Superplasticizer		Cement (kg/m^3)	SF		Effective water/ binder ratio
			(%)	(kg/m^3)		(%)	(kg/m^3)	
202.5	801	890	0.9	4.05	450 427.5 405	0 5 10	0 22.5 45	0.45

(a) (b)

Fig. 5. Magnetizing of concrete specimens, (a) cube, (b) prism.

2.4. Durability properties

For the first time, to the best of our knowledge, the present study investigated experimentally the effect of applying MF with flux densities of 0.5, 0.8, and 1 T to concrete specimens containing 5% and 10% SF on their durability. To achieve this aim, electrical resistance of concrete, and chloride ion penetration tests were conducted.

2.4.1. Electrical resistance of concrete exposed to MF

The electrical resistance of concrete specimens, as a nondestructive test, was used to assess the corrosion risk of concrete subjected to a corrosive environment using a 4-pin Wenner probe array, as depicted in Fig. 6. The surface resistivity apparatus applies an electrical potential difference at the outer probes of the setup, causing an electric current within the concrete. The resulting potential difference between two inner probes was then measured. The electrical resistivity of concrete specimens can be calculated by considering the affected specimen area, the electrical current and potential difference [47,48]. The electrical resistivity was measured in kilohms-centimeters (kΩ-cm). The electrical resistance depends on the movement of ions such as Na, K, OH, SO_4, and Ca within the pores of the concrete mass, which affects the electric field and the concentration of ions. As presented by Song and Saraswathy [47], the relationship between corrosion risk and resistivity is shown in Table 4.

Table 4. Relation between corrosion risk and resistivity in concrete [48].

Resistivity (kΩ-cm)	Corrosion Risk
Greater than 20	Negligible
10 to 20	Low
5 to 10	High
Less than 5	Very high

Fig. 6. 4-pin Wenner probe for electrical resistance of concrete.

2.4.2. Chloride ion penetration in concrete exposed to MF

In order to investigate durability of concrete exposed to different MF intensities, the chloride ion penetration tests were employed based on two various methods: rapid chloride penetrability test (RCPT) and rapid chloride migration test (RCMT).

2.4.2.1. RCP test

According to ASTM C1202 [49], the RCPT is employed to evaluate the strength of concrete specimens against chloride ions penetration by measuring the amount of electrical current passed through them at 28 days. A 50-mm thickness slice of 100-mm diameter was cut from the middle part of each 100 x 200 mm cylinder concrete specimens. These specimens were transferred to cell

of the device as shown in Fig 7. One face of concrete specimen was in the contact with a sodium hydroxide solution (NaOH) and the other face was in contact with a NaCl. A direct current of 60 volts was used for this test. The power supply has two positive and negative outputs which connected to the lateral electrodes of the cell containing NaOH and NaCl solutions, respectively. The current passing across the concrete specimens was recorded at every 5 minutes over a period of 6 hours. By calculating the area under the current-time graph, the total charge passing through the specimen was measured. The results were the average values of three specimens.

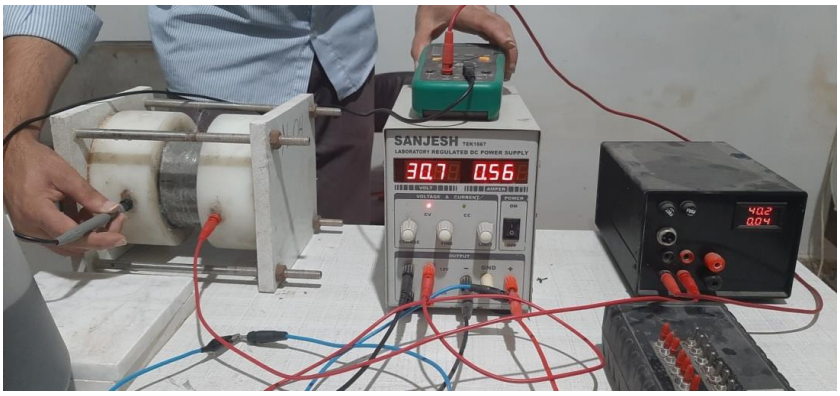

Fig. 7. RCP test setup.

2.4.2.2. RCM test

According to NT Build 492 [50], the RCMT is employed to probe the chloride penetration depth of concrete specimens by applying an external electrical potential to them, leading to migrate the chloride ions outside into the concrete specimens. The process of preparing and properties of specimens used in this test were similar to the RCPT. The surface of the specimens should be dry. They were placed in a rubber sleeve, and their peripheral surfaces were insulated. Then, the rubber sleeve was filled with a 0.3 mol (M) NaOH. All this equipment was placed in a container filled with a 10% NaCl in such a way that the bottom surface of specimen was in the contact with the NaCl solution while the upper surface was in contact with the NaOH solution, as shown in Fig. 8. NaCl and NaOH solutions served as the catholyte and anolyte solutions, respectively. The power supply has two positive and negative outputs which connected to the anode and cathode, respectively. The voltage preset at 30 volts DC power supply and the initial current through specimen was recorded. Test duration was obtained according to NT Build 492 [50]. After that the specimen was removed from the rubber sleeve, rinsed with water and splitted into two halves. The freshly split section was soon sprayed with 0.1 M silver nitrate solution (AGNO3). After about 15 minutes, the white silver chloride precipitation on the mentioned surface will be visible. To measure the depth of chloride ion penetration, depth of the discolored area was measured. Finally, the non–steady-state migration coefficients (Dnssm) were used to investigate the chloride ion penetration of concrete.

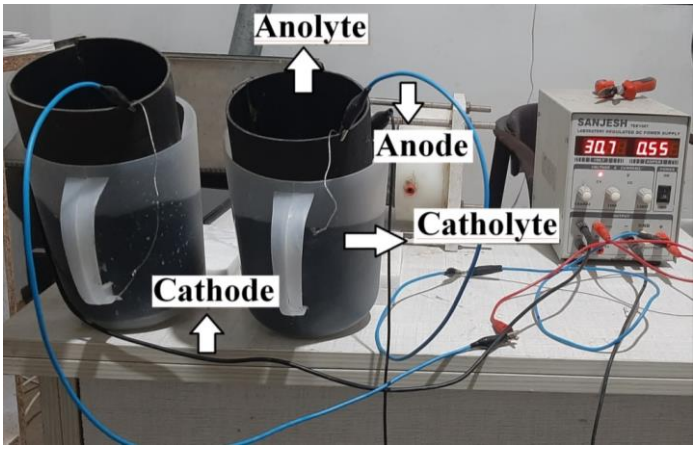

Fig. 8. RCM test setup.

3. Results and discussions

3.1. Compressive strength of concrete exposed to MF

The variation of compressive strength of concrete specimens incorporating 0, 5 and 10% SF under the influence of different MF intensities are shown in Fig. 9. It can be inferred that the applying different MF intensities to fresh concrete increased its mechanical strength. Concerning this, compressive strengths of Mag specimens subjected to MF of 0.5, 0.8 and 1 T were enhanced by 14.7, 16.2 and 17%, respectively, in comparison with N.Mag specimen. In addition, increasing SF content in concrete can enhance its compressive strength. Regarding this, these amounts were obtained for Mag-SF5 specimens up to 18.4, 22.2 and 23.2%, respectively. Also, applying MF of 0.5, 0.8 and 1 T to Mag-SF10 specimens increased their compressive strength by 19.2, 22.3 and 24.2%, respectively, compared to the N.Mag-SF10. According to Fig. 9, it can be stated that the inclusion of 5 and 10% SF in concrete caused a remarkable increase in its compression performance by 20.7 and 33.7%, respectively. Compressive strength results for the concrete specimens exposed to different MF intensities are presented in Table 5.

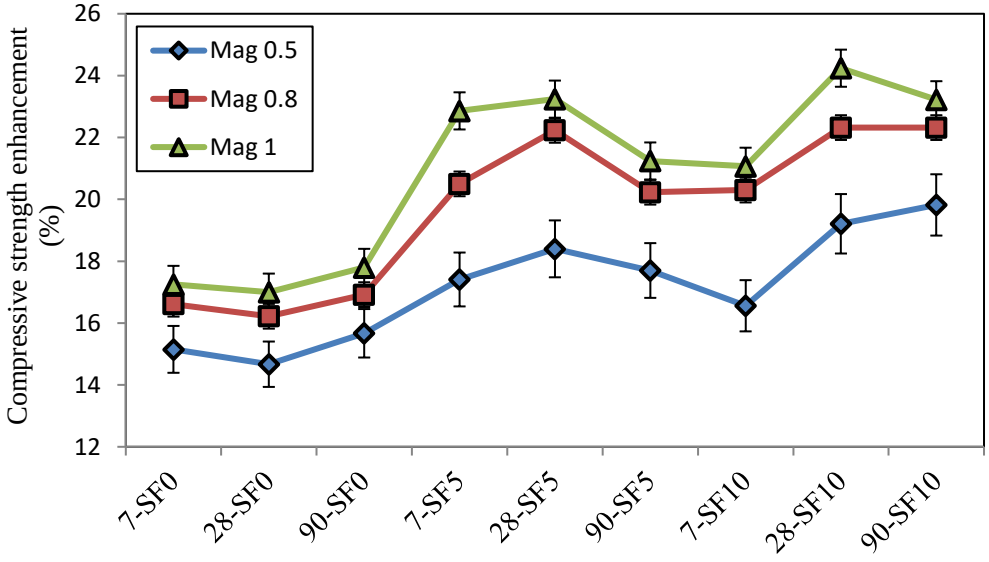

Fig. 9. Variation of compressive strength of concrete exposed to different MF intensities.

The effect of MF on concrete may be due to charged grains in cementitious materials like cement and SF, and also used sand. Exposing concrete to MF caused a significant increase in the amounts of C-S-H with a compacted morphology as showed by Soto-Bernal et al. [22] for cement paste. This manner can reduce the permeability value, and increase compressive strength of concrete. Similar observations were also revealed by Abavisani et al. [23,33] and Hajforoush et al. [24,25]. Besides, the presence of SF in concrete specimens can improve the effectiveness of concrete exposed to MF. There are silicate (SiO_4) and hydroxyl groups (-OH) on the surface of SF particles, which can generate positive or negative charges. A hydroxyl group consists of one hydrogen atom and one oxygen atom. The hydroxyl group is polar, with the oxygen side being always negative, while the hydrogen side is positive. These surface electric charges can cause other particles to be attracted or repelled. According to Villary,s law, SF particles align in the apposite direction of the magnetic flux lines due to their diamagnetic properties when MF is applied to concrete specimens containing SF. This means that the MF can cause movement in the electric charges on the surface of SF particles, altering the attraction and repulsion forces between particles. Consequently, the edhension between SF particles and cement with aggrigates in concrete exposed to MF is strongly enhanced by the formation of new bonds. Additionally, there is a difference in the failure pattern of concrete specimens with SF exposed to the MF. It can be inferred that magnetic flux intensity has a significant effect on the collapse behavior, inducing a brittle failure mode. Increasing the magnetic flux intensity causes to concrete specimens behave more brittle under compressive load. In other words, incresing MF intensity caused an enhance in mechanical strength and also a reduce in porosity content of concrete specimens incorporating SF.

Table 5. Compression test results for concrete exposed to different MF intensities.

Specimen	MF intensity (T)	Age (day)	Compressive strength (MPa)	Enhancement (%)	Standard deviation (MPa)
N.Mag	0	7	23.75	-	4.8
Mag	0.5	7	27.35	15.15	3.9
Mag	0.8	7	27.69	16.61	3.1
Mag	1	7	27.85	17.25	3.5
N.Mag-SF5	0	7	26.98	-	4.5
Mag-SF5	0.5	7	31.68	17.41	4.1
Mag-SF5	0.8	7	32.51	20.5	3.2
Mag-SF5	1	7	33.15	22.86	3.6
N.Mag-SF10	0	7	29.06	-	4.5
Mag-SF10	0.5	7	33.87	16.56	4.3
Mag-SF10	0.8	7	34.96	20.3	3.7
Mag-SF10	1	7	35.18	21.07	4.2
N.Mag	0	28	31.17	-	3.9
Mag	0.5	28	35.74	14.67	3.6
Mag	0.8	28	36.23	16.22	2.6
Mag	1	28	36.47	17	2.9
N.Mag-SF5	0	28	37.61	-	4
Mag-SF5	0.5	28	44.53	18.4	3.5
Mag-SF5	0.8	28	45.97	22.23	2.8
Mag-SF5	1	28	46.35	23.24	3.1
N.Mag-SF10	0	28	41.67	-	4.2
Mag-SF10	0.5	28	49.67	19.21	3.9
Mag-SF10	0.8	28	50.97	22.32	2.8
Mag-SF10	1	28	51.77	24.24	3.6
N.Mag	0	90	34.33	-	4.6
Mag	0.5	90	39.71	15.67	4.1
Mag	0.8	90	40.14	16.92	3.4
Mag	1	90	40.44	17.8	3.8
N.Mag-SF5	0	90	44.61	-	4.2
Mag-SF5	0.5	90	52.51	17.7	4
Mag-SF5	0.8	90	53.63	20.23	3.1

Mag-SF5	1	90	54.09	21.24	3.5
N.Mag-SF10	0	90	48.67	-	4.8
Mag-SF10	0.5	90	58.32	19.82	4.1
Mag-SF10	0.8	90	59.53	22.32	3.3
Mag-SF10	1	90	59.97	23.22	3.8

3.2. Flexural strength of concrete exposed to MF

Fig. 10 indicates the results of flexural strength of concrete with 0, 5 and 10% SF, subjected to the different MF intensities. Following this, flexural strengths of Mag samples under MF of 0.5, 0.8 and 1 T were enhanced by 7.1, 7.1 and 8.5%, respectively, in comprison with N.Mag specimens. In addition, applying MF with the abovementioned intensities to Mag-SF5 specimen caused an increase in their flexural strengths up to 9.7, 11 and 12.1%, respectively. These amounts for Mag-SF10 specimen were obtained 11.4, 12.4 and 14.6%, respectively. It means that by increasing the MF intensity, and subsequently rising the temperature of the specimens, cement hydration reaction is accelerated so a molecular restructuring process is occurred in the specimens, leading to a decrease in the permeability value of the specimens. In addition, the presence of SF as diamagnetic particles in concrete may increase its flexural performance by more susceptibility of the concrete under MF. Hence, the bond strength between hydrated cement paste and SF particles increased strongly. Therefore, the flexural strength of concrete exposed to MF is enhanced. The same results was also obtained by Soto-Bernal et al. [22] for cement pastes under the influence of weak MFs and also by Mu et al. [51]. Furthermore, SEM analysis showed that MF can reduce calcium hydroxide during the cement hydration process, converting it into C-S-H gel. This gel is essential for the development of mechanical strength in concrete.

As per Fig. 10, it can be seen that the increasing the SF content in concrete increased its flexural strength. The incorporation of 5 and 10% SF into concrete increased its flexural strength to 2.6 and 11.5%, respectively. Besides, flexural strength of Mag specimen increased by 2.5% due to an increase in the SF content. The results of flexural strength of concrete were almost similar to what obtained for compressive strength as showed by Hosseini et al. [52–54] for concrete.

Fig. 11 is shown the relationship between mechanical strengths of concrete subjected to the different MF intensities. Following this, the equation of $f_r=0.75(f'_c)^{0.5}$ has been developed to assess the flexural strength of concrete with SF under MF based on its compressive strength results where a high correlation coefficient of $R^2=0.92$ was obtained by curve fitting. The values calculated using this equation show strong agreement with ACI 318-19 [40] predictions. The flexural strength for a plain concrete is calculated by Eq. (7) with respect to ACI 318-19 code [40]. Table 6 indicates the recommended empiracal relationships between mechanical strengths of concrete.

$$f_r = 0.62(f'_c)^{0.5} \quad (7)$$

If the MF is applied to fresh concrete specimens incorporating SF, the Eq. (9) is modified as Eq. (8) as shown below:

$$fr=\sqrt{\alpha}0.62(f'c)0.5 \quad (8)$$

According to the present study, exposing ready mixed concrete containing SF to MF causes to alter f_r presented by ACI 318-19 code [40] to $\sqrt{\alpha}f_r$ where coefficient α is proposed by 1.463. Based on ACI 318-19 [40] recommendations, the cube compressive strengths values of concrete exposed to the MF were normalized to cylindrical strengths equivalents.

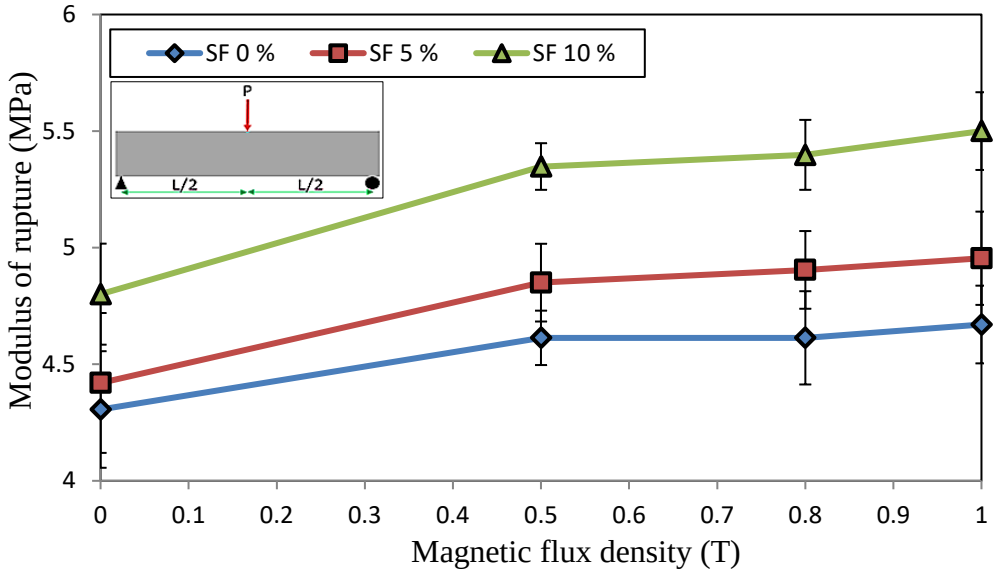

Fig. 10. Flexural strength of concrete specimens exposed to different MF intensities.

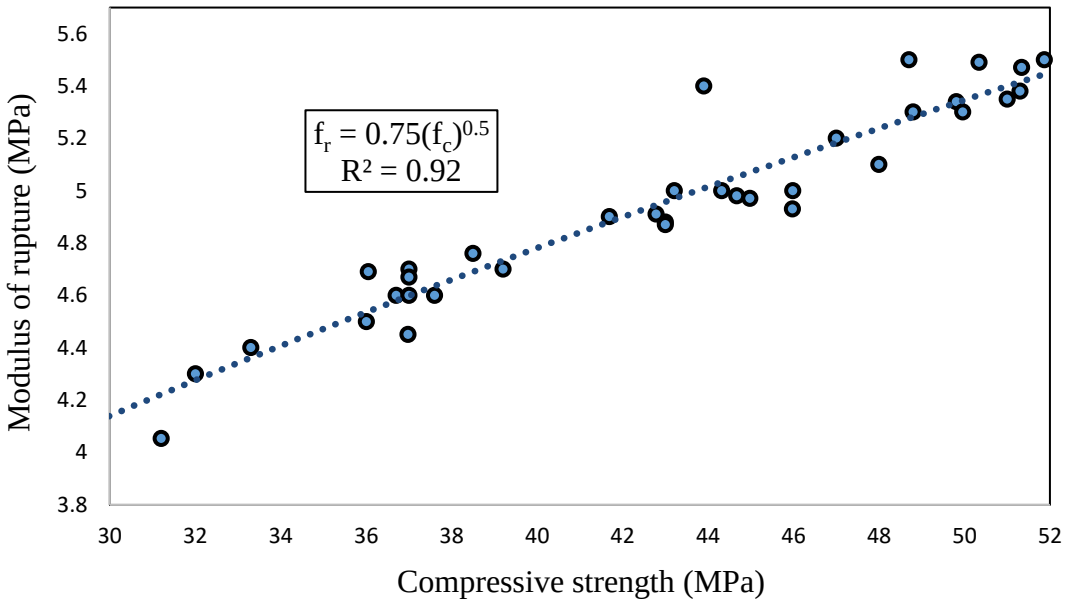

Fig. 11. Variation of mechanical strengths of concrete exposed to different MF intensities.

Table 6. Recommended empiracal relationships between mechanical strengths of concrete.

Reference	Model
IS: 456-2000 [55]	$f_r = 0.7(f_c)^{0.5}$
ACI [40]	$f_r = 0.62(f'_c)^{0.5}$
NZS-3101[56]	$f_r = 0.60(f'_c)^{0.5}$
EC-02 [57]	$f_r = 0.201\ f_c$
BS-8110 [58]	$f_r = 0.60(f'_c)^{0.5}$
Present study	$f_r = 0.75(f'_c)^{0.5}$

3.3. Durability properties of concrete exposed to MF

3.3.1 Electrical resistance of concrete

The values of electrical resistivity of concrete specimens are shown in Fig.12. The results showed that adding SF to concrete caused an increase in its electrical resistance as reported in previous studies [59,60]. Also applying MF to concrete has a same effect. Mag concrete specimens have higher density, less porosity and consequently greater electrical resistance in comparison with the N.Mag concrete specimens. So the risk of Mag concrete corrosion is less than N.Mag specimens. The electrical resistance of all concrete specimens was found to be more than 10 kΩ-cm, which indicates that the corrosion risk is low according to Table 4. It is noteworthy that applying different MF intensities to concrete specimens with 10% SF caused an increase in their electrical resistance to more than 20 kΩ-cm, classifying their corrosion risk as negligible. By escalating the MF from 0 to 1 T caused to an enhance in electrical resistance of concrete specimens containing 0, 5 and 10% SF up to 1.135, 1.159 and 1.183 times, respectively. Also adding 5 and 10% SF to concrete enhanced its electrical resistance up to 25.4 and 46.1%, respectively.

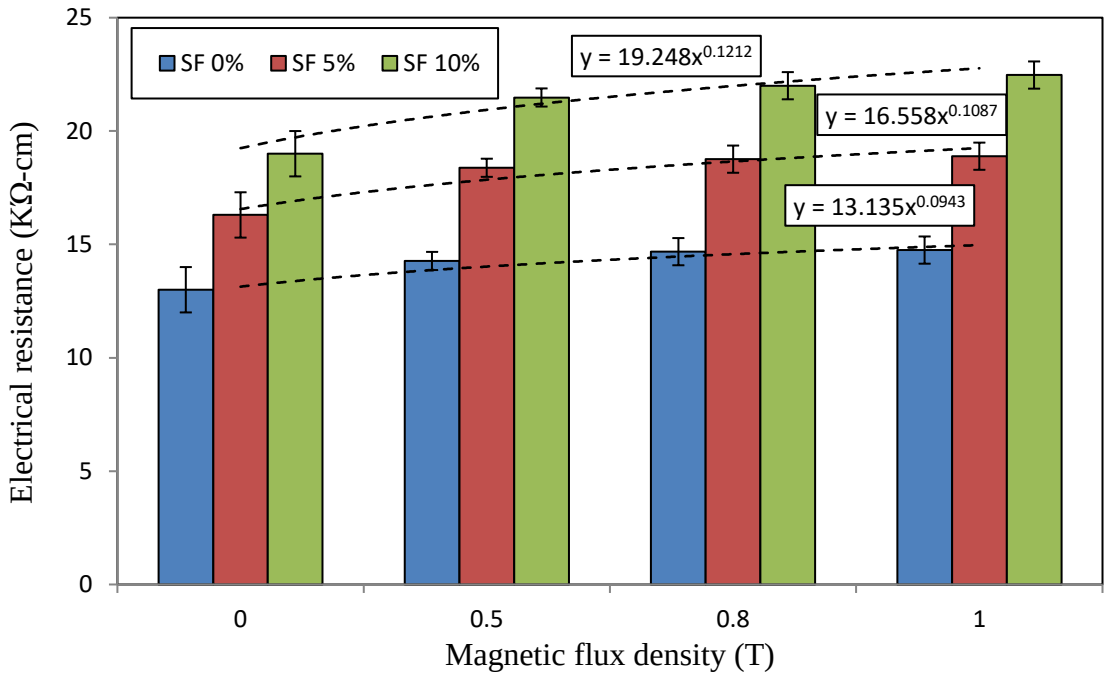

Fig. 12. Electrical resistivity results of concrete specimens exposed to different MF intensities.

3.3.2. Chloride ion penetration

3.3.2.1. RCP test

The effect of applying different MF intensities (0.5, 0.8 and 1 T) and replacement levels of SF (5 and 10%) on chloride ion permeability in concrete specimens resulted from RCPT is shown in Fig. 13. The final recorded passing charge ranged from 4697 to 5308 coulombs for concrete specimens, depending on magnetic flux intensities. These amounts ranged from 1892 to 2203 coulombs and 1017 to 1204 coulombs for concrete specimens with 5 and 10% SF, respectively. N.Mag and Mag concrete specimens were categorized in high chloride ion penetrability, as presented by ASTM C1202 [49]. N.Mag-SF5 concrete specimens were categorized in moderate chloride ion penetrability but Mag-SF5 concrete specimens are categorized in low chloride ion penetrability. Applying MF to concrete specimens incorporating 5% SF can change the risk of

chloride ion penetrability from moderate to low. Also N.Mag and Mag concrete specimens with 10% SF were categorized in low chloride ion penetrability. The presence of SF in concrete can decline the free alkalis content, so adding SF can affect the ionic concentration of the pore solution so chloride permeability decrease [60]. The obtained results are in a good accordance with Bassuoni et al. study [61]. In addition, applying MF to concrete specimens can cause a lower permeability, because Mag specimens have higher density and lower porosity in comparison with N.Mag specimens. By doubling the amount of MF intensity from 0.5 to 1 T, passing charges reduce 4% in concrete specimens containing 10% SF. The present study demonstrated that applying MF to concrete can improve its mechanical properties and durability. Therefore, it is anticipated that the magnetism phenomenon could increase the service life of structures. Based on the concept of life cycle analysis (LCA), which defines the service life of concrete from the time of production until the onset of the first unacceptable damage, the effect of MF on concrete through LCA can be investigated. However, it is evident that, given the increased strength of concrete under the influence of MF, there is a possibility to reduce the amount of cement used, which significantly contributes to reducing greenhouse gas emissions. Regarding this, Su et al. [20,21] showed that the magnetic treatment can reduce the cement consumption in concrete by 5%.

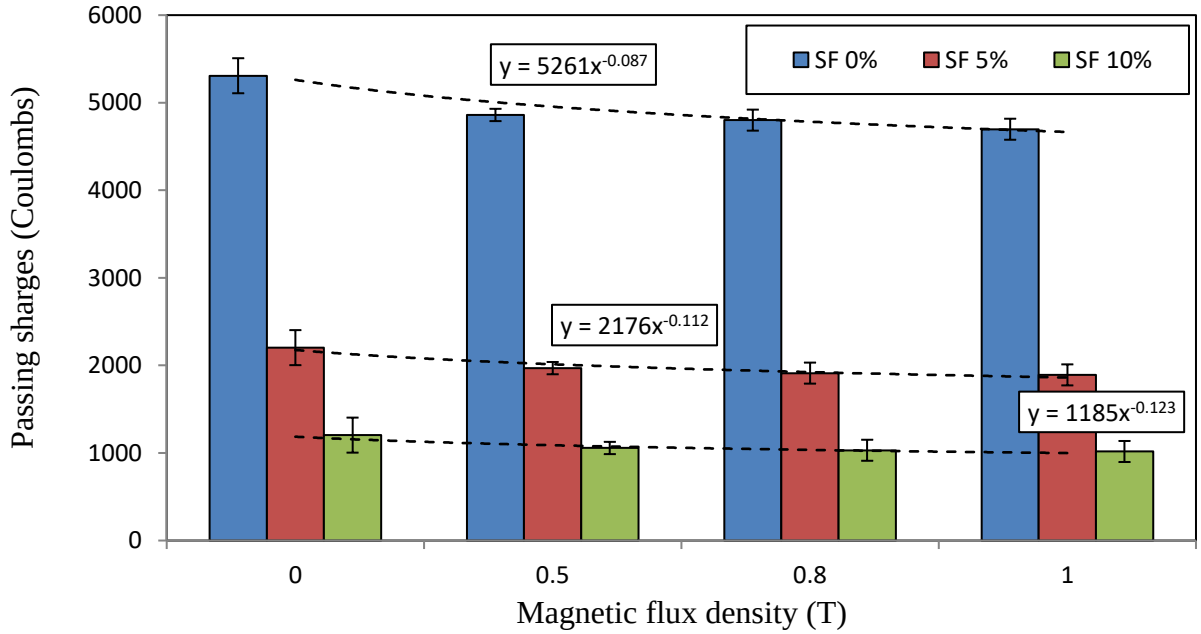

Fig. 13. Effect of applying different MF intensities on passing charges in RCP test.

3.3.2.2. RCM test

The chloride penetration depth measured through 28-day concrete specimens containing different percentages of SF, and affected by the different MF intensities is shown in Fig.14. Depths of chloride penetration for concrete specimens exposed to MFs were in a range of 11.63-13 mm, depending on the intensity of MF where they were in a good accordance with Guneyisi and Mermerdaş study [62]. These amounts were in a range of 8.61-10 mm and 6.6-7.8 mm for concrete specimens containing 5 and 10% SF, respectively. The results showed that concrete specimens with SF had lower chloride penetration depths in comparison with normal specimens. It means that the chloride penetration resistance of the specimens was enhanced by adding 5 and 10% SF to them. This notable improvement can be due to a potential enhancement in the porous structure and changes in the composition of pore solution [63,64]. These modifications may influence the interactions between the migration of chloride and ionic species [65]. Concerning

this, as the MF intensities increased, the chloride penetration depths decreased. The porosity of concrete specimens was reduced due to applying MF to them, so the quality of concrete specimens was improved and accordingly depths of chloride penetration decreased. According to NT Build 492 [50], non-steady-state migration coefficient for concrete exposed to a chloride environment can be calculated by Eq. (9) as shown below:

$$Dnssm = \frac{0.0239\,(273+T)L}{(U-2)t}\,[\,Xd - 0.0238\,\sqrt{\frac{(273+T)L\,Xd}{U-2}}\,] \quad (9)$$

where D_{nssm} is non-steady-state migration coefficient, $\times 10^{-12}$ m^2/s; T is average value of the initial and final temperatures in the anolyte solution (°C), L is thickness of the specimen (mm), U is absolute value of the applied voltage (V), t is test duration (hour), X_d is average value of the penetration depths (mm). In the present study, T is 20 °C, L is 50 mm, U is 30 v and t is 24 h. Fig.15 shows the variation in chloride ion non-steady-state migration coefficient (Dnssm) of concrete specimens exposed to different MF intensities.

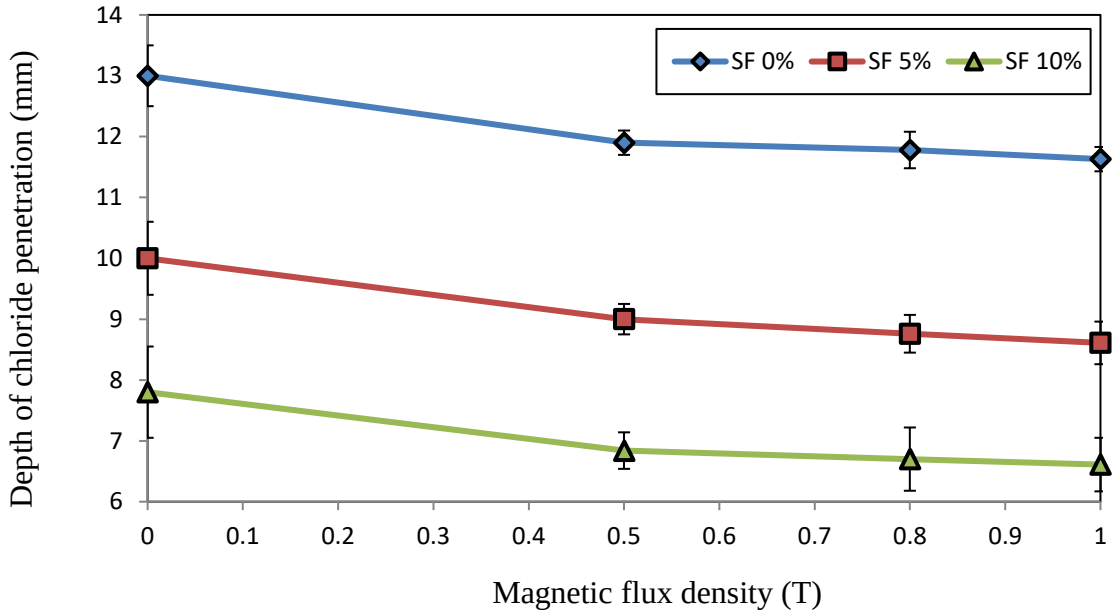

Fig. 14. Variation in chloride ion penetration depth for concrete specimens exposed to different MF intensities.

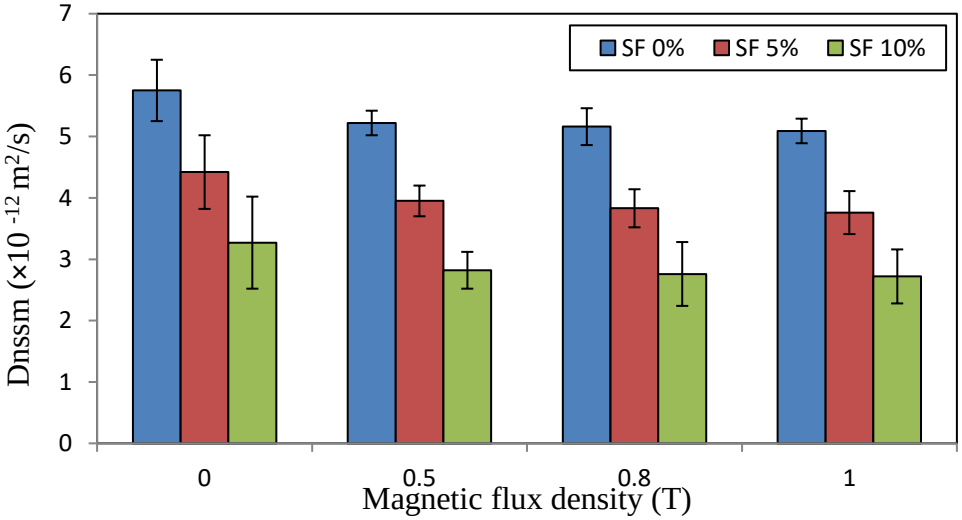

Fig. 15. Variation in chloride ion migration coefficient for concrete specimens exposed to different MF intensities.

3.4. Microstructure of concrete exposed to MF

The microscopic images correspond to the N.Mag and Mag specimens with and without SF are shown in Figs. 16(a) to 16(d), respectively. There is a remarkable difference in both the amount and morphology of C-S-H, which is essential for the development of mechanical strength in cementitious composites. Concerning this, the amount of C-S-H gel increases in the presence of the MF in both plain concrete and concrete with SF. In addition, the morphology of the gel becomes denser and less porous compared to the N.Mag specimen. The same behavior was also reported by many researchers such as Soto-Bernal et al. [22], Hajforoush et al. [32,33] and Javahershenas et al. [34] . It can be inferred that MF can decrease the amount of $Ca(OH)_2$ during the cement hydration process, converting it into C-S-H, which is crucial for the development of mechanical strength in cementitious composites. Moreover, Mag specimens have better continuity between fine aggregates and cement paste when compared to the N.Mag specimens. This development in continuity and deduction in porosity may contribute to enhanced concrete mechanical strength and a declined risk of corrosion in concrete specimens as presented in Sec. 4. As per Fig. 14, chemical reactions of cement hydration increased using MF. This can be attributed to the MF promoting the formation of more crystalline phases during the crystallization process. Following this, exposing fresh concrete specimen to the MF reduced $Ca(OH)_2$, which is known to weaken the mechanical strength of cementitious composites. Additionally, the MF facilitates the transformation of calcium hydroxide into C-S-H. These factors may significantly contribute to improved mechanical properties and durability of concrete exposed to MF.

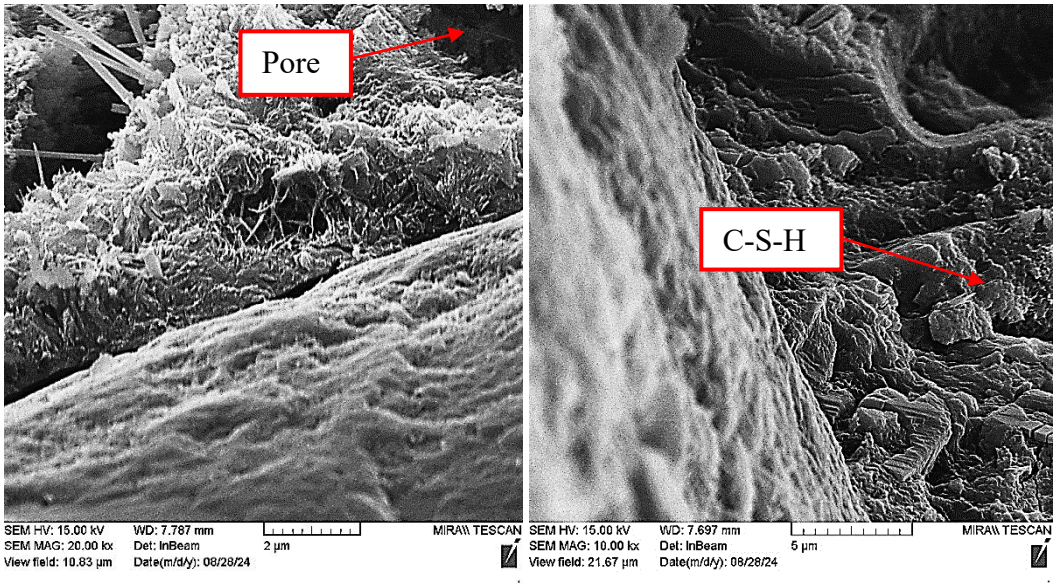

(a) (b)

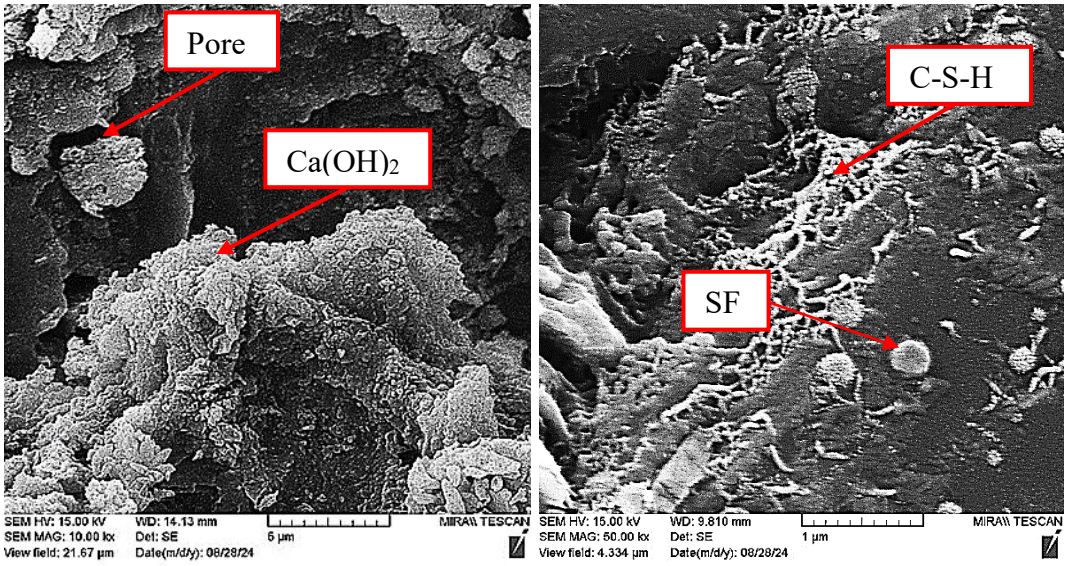

(c) (d)

Fig. 16. Microstructure of concrete by means of SEM imaging, (a) N.Mag, (b) Mag, (c) N.Mag-SF10, (d) Mag-SF10.

4. Conclusions

For the first time, to the best of our knowledge, this research investigated durability of concrete exposed to the different MF intensities in a chloride environment. The study aims to utilize MFs to improve the durability of concrete containing SF in aggressive environments. Following this, the mechanical, durability and microstructural properties of concrete specimens incorporating 5 and 10% SF, which were exposed to the different MF intensitis (0.5-1 T) were evaluated. Based on the present investigation, the following conclusions can be exploited:

- The presence of SF with silicate and hydroxyl groups on its surface led to an increase in the effectiveness of concrete under the influence of MF. Consequently, exposing the Mag-SF10 concrete specimens to a 1 T MF enhanced their compressive and flexural strengths by about 24% and 15%, respectively.
- By rising the MF intensities to 1 T, the depth of chloride penetration of the Mag-SF10 concrete specimens decreased by 15%.
- The electrical and chloride ions penetration resistances of the Mag-SF10 concrete specimens subjected to 1 T of MF increased by 18% and 16%, respectively.
- The SEM analysis showed that the presence of MF leads to better compaction in the cement matrix. This improvement in continuity and reduction in porosity may contribute to enhanced mechanical strength of the concrete and a decreased risk of corrosion in concrete subjected to aggressive environments.

The authors propose investigating the influence of MFs on geopolymer concrete containing diamagnetic materials (e.g., magnetite powder or aggregate). Additionally, applying different MF intensities to high-performance concrete is crucial due to the elevated cement content. Furthermore, it is anticipated that the magnetism phenomenon can increase the service life of structures. Based on the concept of LCA, the authors suggest that the effect of MF on concrete through LCA can be investigated.

Funding

This research did not receive any specific grant from funding agencies in the public, commercial, or not-for-profit sectors.

Conflicts of interest

The authors declare that they have no known competing financial interests or personal relationships that could have appeared to influence the work reported in this paper.

Authors contribution statement

Fakhri Javahershenas: Methodology, Investigation, Writing – original draft, Funding acquisition.

Malek Mohammad Ranjbar: Supervision, Writing – review & editing.

Morteza Sohrabi Gilani: Supervision, Writing – review & editing.

Mohammad Hajforoush: Conceptualization, Methodology, Writing – review & editing.

References

[1] Raza SS, Amir MT, Azab M, Ali B, Abdallah M, El Ouni MH, et al. Effect of micro-silica on the physical, tensile, and load-deflection characteristics of micro fiber-reinforced high-performance concrete (HPC). Case Stud Constr Mater 2022;17. https://doi.org/10.1016/j.cscm.2022.e01380.

[2] Tayeh BA, Akeed MH, Qaidi S, Bakar BHA. Influence of microsilica and polypropylene fibers on the fresh and mechanical properties of ultra-high performance geopolymer concrete (UHP-GPC). Case Stud Constr Mater 2022;17:e01367.

[3] Haastrup S, Bødker MS, Hansen SR, Yu D, Yue Y. Impact of amorphous micro silica on the C-S-H phase formation in porous calcium silicates. J Non Cryst Solids 2018;481:556–61. https://doi.org/10.1016/j.jnoncrysol.2017.11.051.

[4] Bhagat N. K GJS. Effect of micro-silica and nano-silica on mechanical properties of concrete. Int J Civ Eng Technol 2018;9:1–7.

[5] Potapov VV, Efimenko YV, Gorev DS. Determination of the amount of Ca(OH)2 bound by additive nano-SiO2 in cement matrices. Nanotechnologies Constr A Sci Internet-Journal 2019;11:415–32. https://doi.org/10.15828/2075-8545-2019-11-4-415-432.

[6] Pratap B. Analysis of the synergistic effects of micro silica on the mechanical and durability properties of geopolymer concrete incorporating phosphogypsum. J Build Eng 2024;93:109831.

[7] Pandey A, Kumar B. Effects of rice straw ash and micro silica on mechanical properties of pavement quality concrete. J Build Eng 2019;26:100889.

[8] Çelik Aİ, Özkılıç YO, Bahrami A, Hakeem IY. Mechanical performance of geopolymer concrete with micro silica fume and waste steel lathe scraps. Case Stud Constr Mater 2023;19:e02548.

[9] Garg R, Garg R, Singla S. Experimental investigation of electrochemical corrosion and chloride penetration of concrete incorporating colloidal nanosilica and silica fume. J Electrochem Sci Technol 2021;12:440–52.

[10] Ahmad S, Al-Amoudi OSB, Khan SMS, Maslehuddin M. Effect of silica fume inclusion on the strength, shrinkage and durability characteristics of natural pozzolan-based cement concrete. Case Stud Constr Mater 2022;17:e01255.

[11] Eftekhar Afzali S, Ghasemi M, Rahimiratki A, Mehdizadeh B, Yousefieh N, Asgharnia M. Compaction and Compression Behavior of Waste Materials and Fiber-Reinforced Cement-Treated Sand. J Struct Des Constr Pract 2025;30. https://doi.org/10.1061/JSDCCC.SCENG-1643.

[12] Mehdizadeh Miyandehi B, Vessalas K, Castel A MM. Investigation of carbonation behaviour in high-volume ggbfs concrete for rigid road pavements. ASCP (Australian Soc Concr Pavements) 2023.

[13] Esfahani AR, Reisi M, Mohr B. Magnetized water effect on compressive strength and dosage of

superplasticizers and water in self-compacting concrete. J Mater Civ Eng 2018;30:4018008.

[14] Ghorbani S, Ghorbani S, Tao Z, De Brito J, Tavakkolizadeh M. Effect of magnetized water on foam stability and compressive strength of foam concrete. Constr Build Mater 2019;197:280–90.

[15] Hajforoush M, Madandoust R, Kazemi M. Effects of simultaneous utilization of natural zeolite and magnetic water on engineering properties of self-compacting concrete. Asian J Civ Eng 2019;20:289–300.

[16] Hamed YR, Yousry Elshikh MM, Elshami AA, Matthana MHS, Youssf O. Mechanical properties of fly ash and silica fume based geopolymer concrete made with magnetized water activator. Constr Build Mater 2024;411:134376. https://doi.org/10.1016/j.conbuildmat.2023.134376.

[17] Reddy BSK, Ghorpade VG, Rao HS. Effect of magnetic field exposure time on workability and compressive strength of magnetic water concrete. Int J Adv Eng Technol 2013;4:120–2.

[18] Cai R, Yang H, He J, Zhu W. The effects of magnetic fields on water molecular hydrogen bonds. J Mol Struct 2009;938:15–9.

[19] Gholhaki M, Hajforoush M, Kazemi M. An investigation on the fresh and hardened properties of self-compacting concrete incorporating magnetic water with various pozzolanic materials. Constr Build Mater 2018;158:173–80.

[20] Su N, Wu Y-H, Mar C-Y. Effect of magnetic water on the engineering properties of concrete containing granulated blast-furnace slag. Cem Concr Res 2000;30:599–605.

[21] Su N, Wu C-F. Effect of magnetic field treated water on mortar and concrete containing fly ash. Cem Concr Compos 2003;25:681–8.

[22] Soto-Bernal JJ, Gonzalez-Mota R, Rosales-Candelas I, Ortiz-Lozano JA. Effects of static magnetic fields on the physical, mechanical, and microstructural properties of cement pastes. Adv Mater Sci Eng 2015;2015:934195.

[23] Abavisani I, Rezaifar O, Kheyroddin A. Alternating magnetic field effect on fine-aggregate steel chip–reinforced concrete properties. J Mater Civ Eng 2018;30:4018087.

[24] Ferrández D, Saiz P, Morón C, Dorado MG, Morón A. Inductive method for the orientation of steel fibers in recycled mortars. Constr Build Mater 2019;222:243–53.

[25] Abavisani I, Rezaifar O, Kheyroddin A. Alternating magnetic field effect on fine-aggregate concrete compressive strength. Constr Build Mater 2017;134:83–90.

[26] Abavisani I, Rezaifar O, Kheyroddin A. Magneto-electric control of scaled-down reinforced concrete beams. ACI Struct J 2017;114:233–44.

[27] Rezaifar O, Abavisani I, Kheyroddin A. Magneto-electric active control of scaled-down reinforced concrete columns. ACI Struct J 2017;114:1351–62.

[28] Zieliński M. Influence of constant magnetic field on the properties of waste phosphogypsum and fly ash composites. Constr Build Mater 2015;89:13–24.

[29] Tarbozagh AS, Rezaifar O, Gholhaki M. Electromagnetism in taking concrete behavior on demand. Structures, vol. 27, Elsevier; 2020, p. 1057–65.

[30] Tarbozagh AS, Rezaifar O, Gholhaki M, Abavisani I. Magnetic enhancement of carbon nanotube concrete compressive behavior. Constr Build Mater 2020;262:120772.

[31] Hajforoush M, Kheyroddin A, Rezaifar O. Investigation of engineering properties of steel fiber reinforced concrete exposed to homogeneous magnetic field. Constr Build Mater 2020;252:119064.

[32] Hajforoush M, Kheyroddin A, Rezaifar O, Kioumarsi M. The effects of uniform magnetic field on the mechanical and microstructural properties of concrete incorporating steel fibers. Sci Iran 2021;28:2557–67.

[33] Hajforoush M, Kheyroddin A, Rezaifar O, Kazemi M. Magnetic field effect on bond performance between reinforcement and concrete containing steel fibers. J Build Eng 2024;98:111215.

[34] Javahershenas F, Gilani MS, Hajforoush M. Effect of magnetic field exposure time on mechanical and microstructure properties of steel fiber-reinforced concrete (SFRC). J Build Eng 2021;35:101975.

[35] Xue W, Chen J, Xie F, Feng B. Orientation of steel fibers in magnetically driven concrete and mortar. Materials (Basel) 2018;11:170.

[36] Chen J, Wang J, Jin W. Study of magnetically driven concrete. Constr Build Mater 2016;121:53–9.

[37] Amini MM, Ghanepour M, Rezaifar O. Experimental analysis of the impact of alternating magnetic fields

on the compressive strength of concrete with various silica sand and microsilica compositions. Case Stud Constr Mater 2024;21:e03487.

[38] Rezaifar O, Ghanepour M, Amini MM. A novel magnetic approach to improve compressive strength and magnetization of concrete containing nano silica and steel fibers. J Build Eng 2024;91:109342.

[39] Ahmed SM, Manar DF. Effect of static magnetic field treatment on fresh concrete and water reduction potential. Case Stud Constr Mater 2021;14:e00535.

[40] Institute AC. ACI. Building code requirements for structural concrete and commentary. ACI 318-19. Farmington Hills, MI, USA: 2019.

[41] ASTM International. ASTM C150 / C150M-19a Standard Specification for Portland Cement. Annu B ASTM Stand 2019:2019.

[42] ASTM C33, (2018). Standard Specification for Concrete Aggregates, ASTM International West Conshohocken. 2018:2018.

[43] ASTM International. ASTM D1129-13. Standard Terminology Relating to Water. West Conshohocken, PA.: 2013.

[44] ASTM International. ASTM C494. Standard Specification for Chemical Admixtures for Concrete. West Conshohocken, PA, USA.: 2004.

[45] Grant IS, Phillips WR. Electromagnetism. John Wiley & Sons; 2013.

[46] ASTM C192. Standard Practice for Making and Curing Concrete Test Specimens in the Laboratory (2018). ASTM International, West Conshohocken. PA, USA. 2018:2018.

[47] Song H-W, Saraswathy V. Corrosion Monitoring of Reinforced Concrete Structures – A Review. Int J Electrochem Sci 2007;2:1–28. https://doi.org/10.1016/S1452-3981(23)17049-0.

[48] AASHTO T95. Standard Method of Test for Surface Resistivity Indication of Concrete's Ability to Resist Chloride Ion Penetration . AASHTO Provisional Stand 2011:3–5.

[49] ASTM International. ASTM C1202–05. Test method for electrical indication of concrete's ability to resist chloride ion penetration, Annual Book of ASTM Standards. 2006.

[50] Nordtest method. NT BUILD 942: Concrete , Mortar and Cement-Based Repair Materials : CHLORIDE MIGRATION COEFFICIENT FROM NON-STEADY-STATE MIGRATION EXPERIMENTS. Measurement 1999:1–8.

[51] Mu R, Li H, Qing L, Lin J, Zhao Q. Aligning steel fibers in cement mortar using electro-magnetic field. Constr Build Mater 2017;131:309–16.

[52] Hosseini P, Kaveh A, Naghian A AA. Eco-friendly building solutions: integrating mahallat's travertine sludge in concrete production. Int J Optim Civ Eng 2024;14:229–52. https://doi.org/doi.org/10.22068/ijoce.2024.14.2.584.

[53] Hosseini P, Kaveh A NA. The Use of Artificial Neural Networks and Metaheuristic Algorithms to Optimize the Compressive Strength of Concrete. Int J Optim Civ Eng 2023;13:327–38. https://doi.org/10.1007/978-3-031-66051-1_3.

[54] Hosseini P, Kaveh A NA. Development and optimization of self-compacting concrete mixes: Insights from artificial neural networks and computational approaches. Int J Optim Civ Eng 2023;13:457–76. https://doi.org/doi.org/10.22068/ijoce.2023.13.4.566.

[55] Standards B of I. Standard, I.:456. Indian standard code of practice for plain and reinforced concrete. New Delhi, India.: 2000.

[56] Zealand SN. Standards New Zealand. Concrete Structures Standard -NZS 3101. New Zealand: 2006.

[57] Eurocode No.2. Design of Concrete Structures, Part I, General rules and rules for buildings (2002). Final Draft. 2002:2002.

[58] Institution BS. BS 8110. Structural use of concrete. London: 1985.

[59] Hou J, Chung DDL. Effect of admixtures in concrete on the corrosion resistance of steel reinforced concrete. Corros Sci 2000;42:1489–507.

[60] Shi C. Effect of mixing proportions of concrete on its electrical conductivity and the rapid chloride permeability test (ASTM C1202 or ASSHTO T277) results. Cem Concr Res 2004;34:537–45.

[61] Bassuoni MT, Nehdi ML, Greenough TR. Enhancing the reliability of evaluating chloride ingress in

concrete using the ASTM C 1202 rapid chloride penetrability test. ASTM International West Conshohocken, PA, USA; 2006.

[62] Güneyisi E, Mermerdaş K. Comparative study on strength, sorptivity, and chloride ingress characteristics of air-cured and water-cured concretes modified with metakaolin. Mater Struct 2007;40:1161–71.

[63] Real S, Bogas JA, Pontes J. Chloride migration in structural lightweight aggregate concrete produced with different binders. Constr Build Mater 2015;98:425–36.

[64] Youm K-S, Moon J, Cho J-Y, Kim JJ. Experimental study on strength and durability of lightweight aggregate concrete containing silica fume. Constr Build Mater 2016;114:517–27.

[65] Pontes J, Bogas JA, Real S, Silva A. The rapid chloride migration test in assessing the chloride penetration resistance of normal and lightweight concrete. Appl Sci 2021;11:7251.